ELSEVIER

Thermochimica Acta 291 (1997) 155–169

thermochimica acta

The low-temperature reaction of ferrous sulphide with sulphur dioxide

Andrew K. Galwey[1*]

School of Chemistry, The Queen's University of Belfast, Belfast BT9 5AG, Northern Ireland, UK

Received 16 September 1996; accepted 2 November 1996

Abstract

A kinetic study of a reaction between iron sulphide and sulphur dioxide, 560–700 K, is reported. The measured stoichiometry is summarized:

$$1.00FeS + 0.13SO_2 \rightarrow 0.38Fe_2S_3 + 0.07Fe_3O_4$$

The reaction is strongly deceleratory, α–time data are well expressed by the Jander equation with an activation energy 75±4 kJ mol^{-1}. These results are ascribed to a Wagner parabolic oxidation mechanism controlled by Fe^{3+}-ion diffusion across a barrier layer of product Fe_2S_3. It appears that a porous layer of Fe_3O_4 small crystals is formed on the outer surfaces, accommodating oxide ions resulting from dissociative adsorption of SO_2 with an acceptance of sulphur into the Fe_2S_3 phase.

The rapid reaction of FeS with SO_2, particularly during the early stages, identifies this as being of potential interest, worthy of investigation as a route for the removal of this precursor to acid rain from flue gases. The present results indicate that more work would be required to determine whether the reaction can be usefully applied in environmental protection.

Keywords: Acid rain; Iron sulphide reaction; Solid–Gas reaction; Sulphurdioxide reaction; Wagner solid oxidation

1. Introduction

Sulphur dioxide reacts with ferrous sulphide in the 560–700 K temperature r ange by a deceleratory rate process that yields no gaseous product. The present article reports results of a kinetic and mechanistic study of this reaction, which does not appear to have been identified previously. The chemistry of the iron sulphides and their interactions with sulphur-containing gaseous reactants, such as S_2, SO_2, SO_3 and also O_2, has been the subject of a particularly prolonged and extensive interest. Sulphur-iron compounds first attracted attention during the emergence of chemical science as a distinct discipline. These substances have since remained at the forefront of the economic aspirations, preoccupations and problems of entrepreneurs from alchemists through geological prospectors (*fool's gold*, FeS_2) to acid rain specialists. Some observers might identify an element of *inverse transmutation* in this changing role of iron sulphides in wealth creation.

*Corresponding author. Tel: 01232-245133; fax: 01232-382117.

[1] Present address: 18, Viewfort Park, Dunmurry, Belfast BT17 9JY, Northern Ireland, UK, Tel: (01232) 611459.

0040-6031/97/$17.00
PII S0040-6031(96)03113-9

The literature concerned with reactions between Fe/S/O compounds is extensive. Reasons for this include the economic importance of these substances, together with the intrinsic interest in the diversity of the solid phases involved, that include Fe, FeS, FeS_2, $FeSO_4$, $Fe_2(SO_4)_3$, together with FeO, Fe_3O_4 and Fe_2O_3 and the various gases with which these react: S_2, SO_2, SO_3, O_2 and others. Inhomogeneities in the reactant solids, including non-stoichiometry, polymorphism and the involvement of two dominant oxidation states in iron (Fe^{2+}, Fe^{3+}; others are possible) makes it desirable that work in this field extends to the characterization of the structures and compositions of reactants, products and any intermediate phases in some detail. These general considerations apply equally to a wide range of other gas–solid reactions, where the interpretation of kinetic observations requires involvement of the specific characteristics of heterogeneous rate processes. Factors influencing the reactivities and kinetic behaviour of rate processes involving solids [1] include particle sizes and shapes, compositional and structural inhomogeneities within, and between reactant particles, diffusion control including the effects of a product barrier layer and melting, which may be local and/or temporary [2]. Overall kinetic characteristics may, in addition, be influenced by equilibria established between participating reactants, e.g. $2SO_3 \leftrightarrow 2SO_2 + O_2$. Thus, the rates of chemical changes involving solids, in addition to the influences of reactant pressures and reaction temperature (as in most chemical processes), may also be sensitive to the properties of the individual crystalline sample of reactant used. There may be irreproducibility of observations between experiments with different preparations of (apparently) the same reactant solid. Stoichiometric, kinetic and mechanistic conclusions for gas–solid reactions must, therefore, recognize the inherent complexities of the chemical changes involved, where more than a single rate process may participate, particularly at high temperatures.

The inherent complexities of reactions involving Fe/S/O compounds are implicitly recognized in research reports, where contributory rate processes are usually conveniently represented by *several* simple, balanced stoichiometric equations. However, apparent chemical inconsistencies are to be discerned in the literature and unresolved problems remain for future investigation. This subject area, notably including solid iron sulphides, would undoubtedly benefit from up-to-date systematic, authoritative and critical reviews of the extensive published material.

The reaction $FeS+SO_2$, reported here, is identified as worthy of attention for two distinct reasons. Scientific interest is concerned with establishing the mechanism of this low-temperature process. The reactions occurring are expected to be most easily interpreted in the absence of the additional concurrent or consecutive processes that become significant as reaction temperature is increased. No gaseous products were detected in this reaction which was studied at temperatures (560–700 K) appreciably below that (770 K) at which the following processes were reported [3] as occurring: $FeS + 2SO_2 \rightarrow FeSO_4 + S_2$, $4FeSO_4 + S \rightarrow 2Fe_2O_3 + 5SO_2$. No literature references directly relating to the present reaction could be found. In the discussion below, our kinetic and stoichiometric observations and mechanistic interpretations are considered in the context of reports of related reactions.

The second reason for interest in this reaction resides in its possible value as a method for flue-gas desulphurization. The effective removal of SO_2 from the gaseous products of large scale coal combustion is important to diminish this contribution to acid rain, that arises as an unwelcome, polluting by-product from industrial electricity generation plants. Any chemical advance that appears to offer a method for increasing the effectiveness, while reducing the costs, of flue-gas desulphurization, merits consideration as a method of diminishing the present impact of acid rain on the environment. The reaction reported here may have some potential value for use in reducing industrial sulphur emissions. Unfortunately, the necessary further developmental work cannot be continued by the present author, who has now retired from the university. This final experimental study, prematurely terminated by factors outside the author's control, completed a kinetic investigation of the $FeS+SO_2$ reaction. These results are reported and a reaction mechanism accounting for the observations is presented. Conclusions are discussed in the context of previous work concerned with the reactions of SO_2 with $CaCO_3$ and $CaSO_3$ [4–6], which provided the background for the present study. The potential value

of the work for environmental protection is also discussed.

2. Experimental

2.1. Apparatus

The conventional glass vacuum apparatus used for kinetic measurements has already been described [7]. Evacuation was by a rotary oil pump backing a two-stage mercury diffusion pump, capable of achieving pressures below 10^{-3} Nm^{-2}. Pressures within the constant gas retention volume (0.88 ℓ) were measured by a Baratron absolute pressure diaphragm gauge, MKS222B, working in the 0–1500 Nm^{-2} pressure range, which were read within ± 0.1 Nm^{-2}. Gauge output, confirmed by direct calibration to be directly proportional to pressure, was recorded at prespecified time intervals and the pressure, time, and temperature values were stored in the controlling computer. Programmes available enabled yield–time data to be tested for the fit to appropriate rate expressions [1] and output facilities permitted the presentation of results in tabular and in graphical forms.

Reactant FeS samples, usually 50–250 mg and individually weighed ± 0.1 mg, were initially evacuated for 30 min before admission of the SO_2 reactant at $\sim$1 500 Nm^{-2}. The pressure, time, and temperature data were recorded during isothermal reactions in the 560–700 K interval. After completion of the reaction, observations were calculated in the form of fractional reaction α–time for examination in the kinetic analysis. The residual solids were cooled in the remaining SO_2 atmosphere (before admission of air) and then immediately weighed.

2.2. Reactant

A single commercially supplied preparation of FeS, manufactured by heating an iron–sulphur mixture, was used throughout the present work. External surfaces and discoloured regions of the large particles were discarded to remove the oxidation products formed during storage. The black solid was crushed and sized by sieving into five fractions of nominal particle size ranges: <63, 63–75, 75–125, 125–250, and >250 μm. Each sample was stored under nitrogen in a tightly stoppered bottle and used within a few days to minimize oxidation before kinetic studies.

Pure SO_2 was obtained from a cylinder (BDH). The gas was introduced into the evacuated apparatus, condensed at 78 K, again evacuated and stored in a 5 l bulb for a short period before use. Oxygen was prepared by decomposition of $KMnO_4$ in vacuum and similarly stored in a 5 l evacuated bulb.

3. Results and discussion

3.1. Reaction stoichiometry

Isothermal kinetic studies used 50–100 mg samples of FeS reacting with 500–1500 Nm^{-2} SO_2 in a 0.88 l containing volume. The pronounced deceleratory character of reaction made it difficult to measure precisely the overall pressure change corresponding to the completion of reaction (α=1.00). From 26 experiments in the 620–720 K range, with reaction times extended up to 40 h at the lower temperatures, it was concluded that 1.00 mol FeS reacted with 0.132 ± 0.002 mol SO_2. No systematic variation with temperature was found. This result is supported by the gravimetric measurements, the average weight increase corresponded to 0.130 ± 0.005 mol SO_2 and appears from the slightly greater scatter of values to be the somewhat less precise of the two measurements.

Gas remaining in the apparatus after reaction was completely condensed at 78 K, confirming that no oxygen product was released. The cooled and evacuated residual solid products yielded no detectable amount of gas on reheating in vacuum to the highest of the present reaction temperatures, 2 h at 720 K. Reactions ($FeS+SO_2$) were not accompanied by sulphur sublimation, the limit of detection being estimated to be less than 1 mg S_2 (below 2% of reactant weight). In a single experiment there was a barely observable yield of sublimed sulphur after heating a sample of crushed reaction product in vacuum for several hours at 720 K. The conditions of this single experiment were more severe than those used in the present kinetic studies.

From the stoichiometric evidence, the reaction of FeS with SO_2 below 720 K can be represented to a

close approximation by

$$1.00FeS + 0.13SO_2 \rightarrow 0.38Fe_2S_3 + 0.07Fe_3O_4. \quad (1)$$

X-ray diffraction evidence confirmed the formation of product Fe_3O_4, together with the presence of FeS in partly reacted material. During reaction, the initially loose particles of the reactant powder underwent sintering to form a hard coherent pellet of product aggregate. This is evidence of mobility of surface participating species and the formation of interparticulate cohesive material.

Equation (1) represents gas uptake most satisfactorily. The amount of sulphur and oxygen accommodated corresponds to only partial oxidation of the iron. Fe_2S_3 is unstable but can be prepared by heating FeS+S at ~720 K [8,9]. This is, therefore, a possible product here, if sulphur is released by dissociative adsorption of SO_2 on the reactant surface [6] and the oxygen is accommodated into the Fe_3O_4. The deceleratory character of reaction can be ascribed to control by a diffusion limitation across the barrier Fe_2S_3 layer developed between SO_2 gas and FeS. The volume of gas reacted is relatively small and well below expectation for reactions yielding iron sulphates.

3.2. Electron microscopy

Electron-microscopy observations are reported here before the kinetic analysis to enable conclusions concerning the textual changes accompanying the reaction to be considered in the interpretation of rate measurements. Samples of reactant, product and partially reacted material (α=~0.5) were examined in a Jeol 35CF scanning electron microscope.

The fractured surfaces of the crushed, unreacted FeS particles were almost entirely composed of featureless, approximately planar faces, often bounded by irregular or curved edges. Occasional imperfections, including cracks and narrow pores were noticed. Photographs are not reproduced because appearances were identical with those of the central regions of fractured, partially reacted material, given below.

In contrast, reacted surfaces were textured in the highly characteristic structure shown in the representative photographs of FeS reacted (α=~0.5) in SO_2 at 660 K, Fig. 1(a,b). The outer surfaces of reacted material were composed of a mass of interconnected, probably twinned platelets believed to be Fe_3O_4, of thickness ~0.1 μm and edge lengths ~1.0 μm.

Some of the same reacted material was lightly crushed, in a pestle and mortar after reaction, to fragment particles and thereby expose internal textures for observation. Typical characteristic surfaces revealed are shown in Fig. 2(a,b). Fractured sections across the reaction zone show the presence of a layer of retextured material adhering to the unchanged FeS that constitutes the particle centres. The product is seen in the upper part of Fig. 2(a), the texture of the lower part is similar to that characteristic of the crushed but unreacted FeS. The solid product, believed to be Fe_2S_3, is seen in greater detail in Fig. 2(b) running diagonally across the photograph and coherently bonded to the unreacted FeS, with which it is in contact. We also note that crushing has resulted in detachment of the outermost layer of fine platelets (Fe_3O_4, Fig. 1) that is absent from this material

The outer zone, regarded as solid products, is seen in section and in greater detail in Fig. 2(b), where the coherent contact occurs diagonally across the photograph. This product appears to be crystalline but also contains pores and small voids.

Figure 3 again shows the same features (as in Fig. 2) but, in addition, there is evidence here for the local onset of subsurface reaction. This has occurred within an intraparticulate hole at the bottom of a pore that provides SO_2 access. These crystal imperfections enable reaction to be initiated within all accessible internal holes and this contribution must be considered in interpreting the reaction geometry of interface development. The most important conclusion reached from the microscopic examinations is that reaction is initiated on all FeS surfaces and results in the appearance of a retextured layer, identified as product Fe_2S_3. This is consistent with the reaction model proposed below, that the solid product constitutes a barrier layer between SO_2 gas and the solid reactant FeS.

3.3. Reaction kinetics

Representative examples of the strongly deceleratory isothermal α–time graphs plots, characteristic of

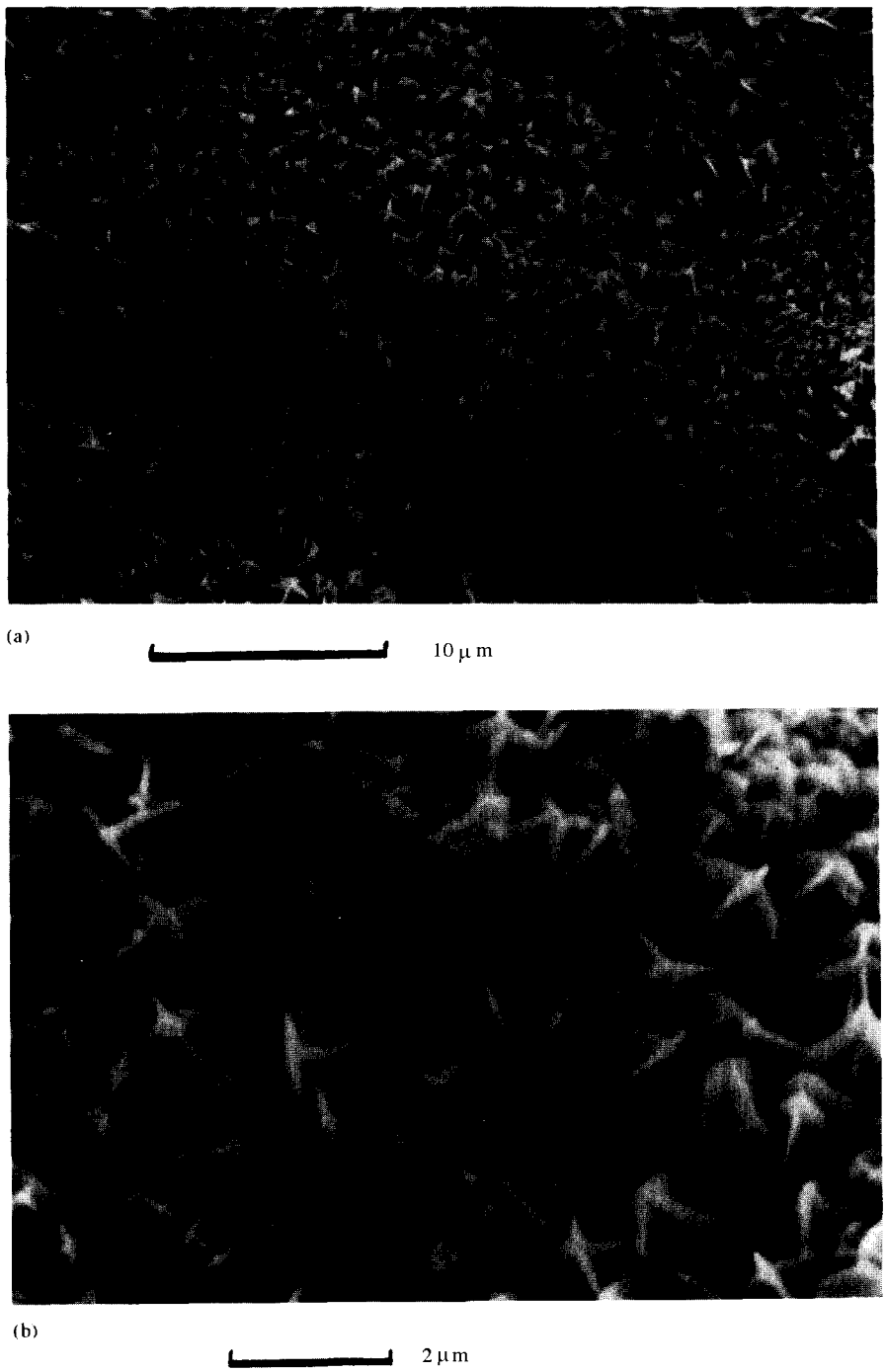

Fig. 1. Typical surface textures of FeS powder particles after reaction to ~50% at 660 K in 1000 Nm^{-2} SO_2. This texture is identified as twinned platelets of Fe_3O_4 and the structure is porous, permitting access of SO_2 to the underlying layer of Fe_2S_3.

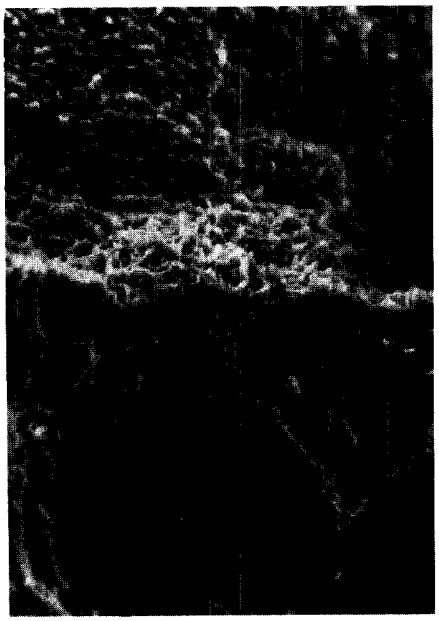

(a)

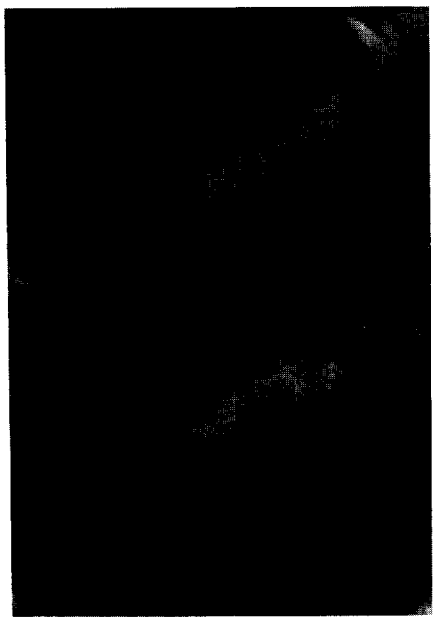

(b)

Fig. 2. Some of the same sample of partly reacted material (α=~0.5) as examined in Fig. 1 was crushed and its typical sections across the outer reaction zones shown here. These (and all other sections examined) gave clear evidence that reaction occurred at all outer boundaries forming a retextured zone believed to be Fe_2S_3. Crushing has apparently detached the outermost restructured layer, which is probably Fe_3O_4 (see Fig. 1). The generally flat surfaces of crystal interiors were similar to those seen for uncrushed, unreacted FeS.

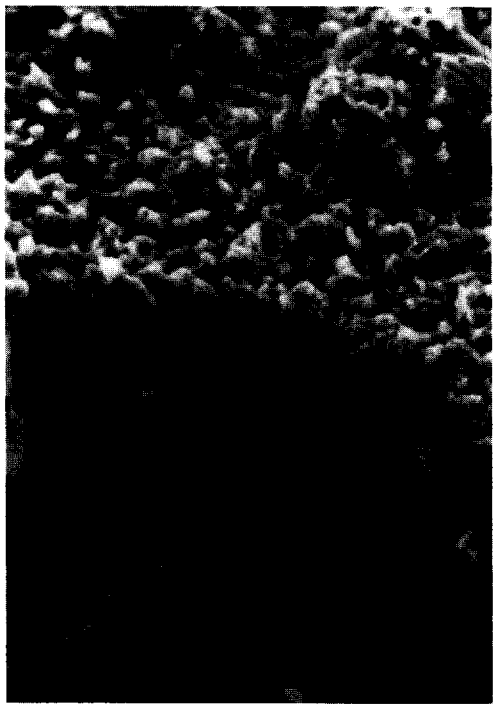

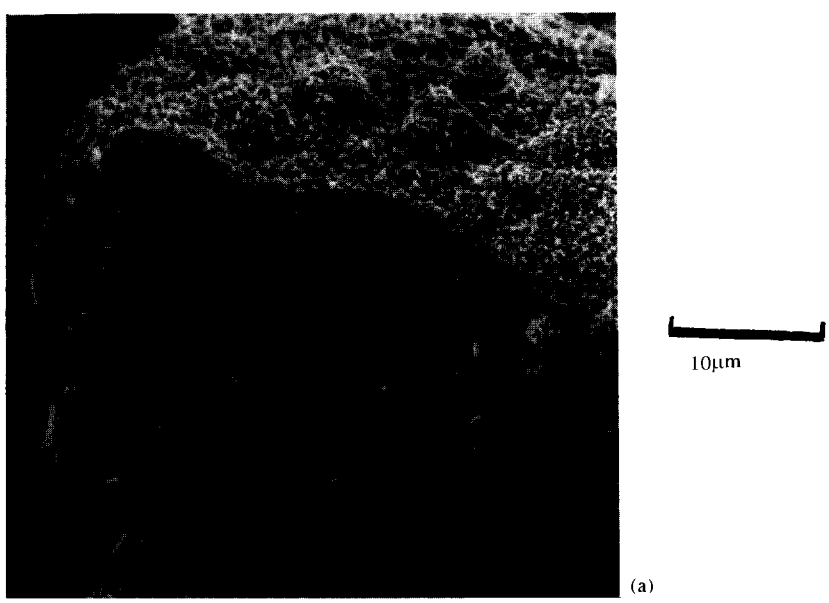

Fig. 3. The retextured boundary surfaces in section are again seen here. In addition, there is onset of reaction well below the surface within an intracrystalline pore space at the end of a channel providing SO_2 access. This is evidence that reaction is initiated at all possible surfaces including some located within these imperfect crystallite assemblages.

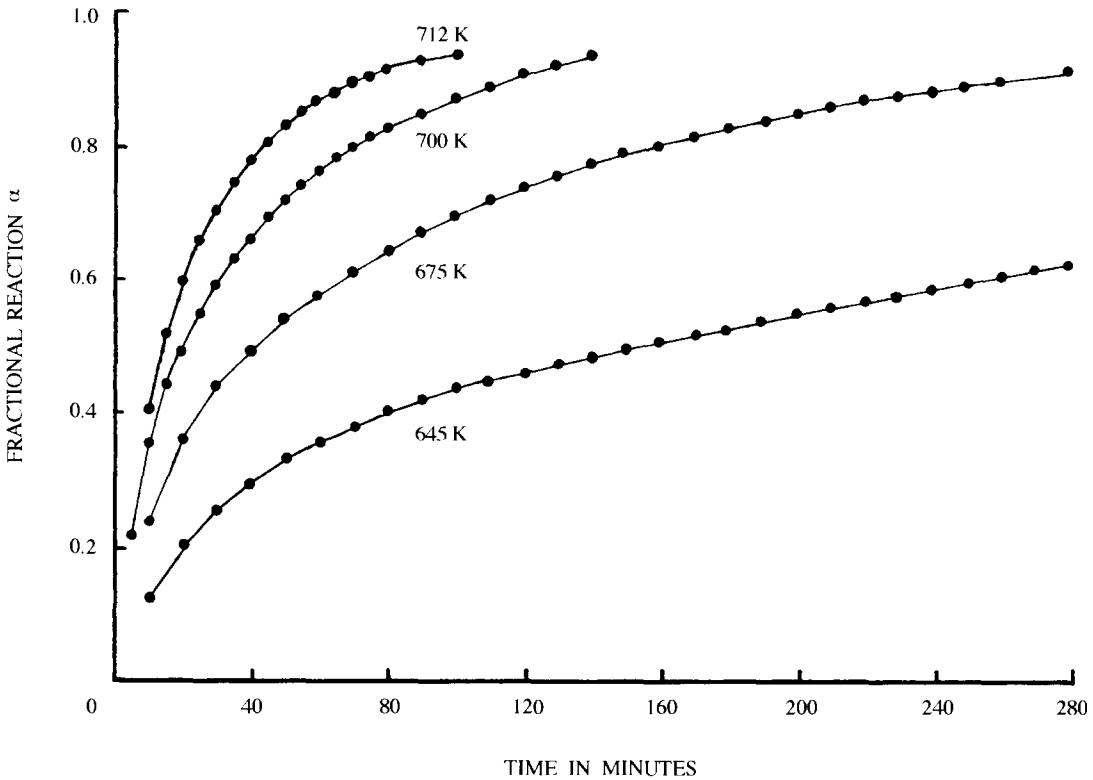

Fig. 4. Four representative isothermal α–time plots for the strongly deceleratory reaction of FeS (sieved, particle sizes 63–75 μm) with SO_2 (700–1000 Nm^{-2} at 645, 675, 700 and 712 K.

reaction (1), are shown in Fig. 4. Kinetic analysis, to identify the best fit [10] of these data to rate equations characteristic of reactions of solids [1], concluded that the Jander expression:

$$[1 - (1 - \alpha)^{1/3}]^2 = kt/r^2 \quad (2)$$

provided the most satisfactory representation (r is the particle radius). This is confirmed by the linearity of plots on Fig. 5 using the same measurements as Fig. 4. All these rate studies were based on measurements of SO_2 pressure reduction for reactions of sieved particles in the size range 63–75 μm (linear dimension). Identifying this as a single rate process, it is concluded that kinetic behaviour is controlled by interface advance into an equidimensional particle subject to control by a diffusion process across a systematically increasing thickness of barrier product layer [11]. This is the Wagner corrosion reaction model [12]. This kinetic conclusion is consistent with the microscopic observations described above.

Rate constants (twelve) determined from experiments including two identically prepared samples of FeS particles agreed, within experimental error, giving a good fit to Eq. (2) when $0.05<\alpha<0.94$. The calculated activation energy was 75 ± 4 kJ mol^{-1}, 557–717 K, for reactions in 700–1000 Nm^{-2} SO_2.

3.3.1. Pressure dependence

The strongly deceleratory character of this reaction made it necessary to measure the dependence of rate on SO_2 pressure by changing this pressure (×2, ×3 or ×0.5) and extrapolating the two sets of rate ($d\alpha/dt$) values to the discontinuity for comparison. The mean pressure dependence of reaction rate, obtained from

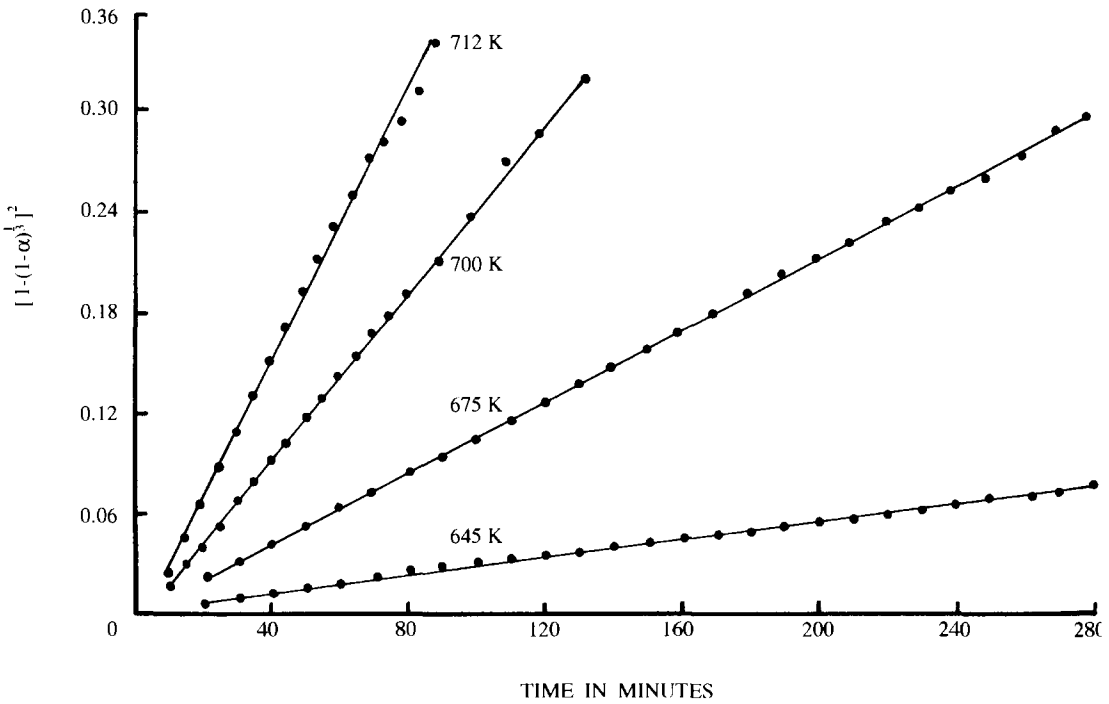

Fig. 5. The α–time data in Fig. 4 are well represented by the Jander equation (2) [1], as shown by these linear plots of $[1-(1-\alpha)^{1/3}]^2$ against time.

14 such comparisons was

$$\text{Rate} \propto P_{SO_2}^{0.5\pm0.1}$$

The effects of reactant pressure change during the isothermal kinetic studies were sought, but not found during rate measurements, generally within the limited 700–1000 Nm^{-2} SO_2 pressure range.

3.3.2. Particle sizes

Rate constants (Eq. (2)) were measured for the reaction of SO_2 with sieved FeS particles within each of the five size ranges separated – (linear dimension)<63, 63–75, 75–125, 125–250, and >250 μm. Relative reaction rates increased systematically with reduction of reactant particle size. Values of k ($=Kr^2$, where K is the measured slope of Jander plots, Fig. 5) were approximately constant for each of the samples of five particle sizes in three series of comparative measurements at 650, 680 and 705 K: mean values of $k(\times 10^{-14}\ m^2\ s^{-1})$ were 1.0±0.3, 2.8±0.7 and 4.7±1.0, respectively. Comparative data from further experiments using single, approximately cube-shaped FeS particles (edge 1.5 mm) reacting at 703 K were again well represented by the Jander equation. The rate of interface advance, $k=5.5\times 10^{-14}\ m^2\ s^{-1}$, was in acceptable agreement with the highest temperature (705 K) value of the foregoing results for powdered reactants.

Within each constant temperature set of comparative kinetic measurements there was a significant tendency for values of k to increase with reactant particle sizes. This is explained by the expected relatively increased probability of a contribution to the overall reaction by chemical change initiated *within* the bulk of the larger particles due to the presence of pores and cracks (see Fig. 3). There was also some uncertainty concerning the reliability of the assumed mean particle sizes, particularly for the finest (<63 μm) and coarsest (>250 μm) powders.

Kinetic studies also included investigations of the effects of crushing partly reacted FeS. Experiments using particles in the larger size ranges were interrupted, cooled in SO_2 and the partially reacted solid was crushed in an agate pestle and mortar. On restoration of the previous reaction conditions, the initial rates were markedly increased, 5–7 times, compared with those measured immediately prior to the interruption. These rates subsequently diminished as the reaction continued. The enhanced rate was ascribed to the rapid initial reaction (Fig. 4) on newly exposed reactive FeS surfaces (Fig. 3) formed during fragmentation by crushing. The deceleratory course of subsequent reaction was similar to the behaviour of a fresh reactant.

All these kinetic results are consistent with a reaction of the type represented in the Jander model [1,11,12]. Reaction of an equidimensional FeS particle proceeds at an interface advancing inwards with rate controlled by a diffusion limitation across an increasing thickness of product layer.

3.4. Reaction of FeS with O_2

Comparative studies were made on the reaction of the present FeS samples with O_2 under similar experimental conditions.

3.4.1. Unreacted FeS: No 78 K trap

The kinetic characteristics of the reaction of $FeS+O_2$ were generally similar to the behaviour reported above for the $FeS+SO_2$ reaction. The deceleratory rate process was well represented by the Jander expression across (at least) the interval $0.1<\alpha<0.85$ and rate constants were close to the same (i.e. $FeS+SO_2$) Arrhenius line. The amount of oxygen that reacted was similar to that of SO_2 but later in the reaction a proportion of the gas present, some 10%, was condensed at 78 K – this is regarded as an evidence of SO_2 formation. Interruption of reaction and evacuation of O_2 before completion, followed by introduction of SO_2, resulted in continuation of gas uptake in accordance with expectation for the final stages of $FeS+SO_2$ reaction.

The kinetic characteristics of reactions of approximately equimolar mixtures of SO_2+O_2 with FeS were again closely similar to the behaviour of the individual gaseous reactants. Reactions were strongly deceleratory and magnitudes of Jander rate constants were comparable. Unfortunately, the composition of the gaseous reactant could not be continually monitored by the present apparatus, though it was confirmed that there was an uptake of both SO_2 and O_2 by the FeS reactant.

3.4.2. Unreacted FeS: 78 K trap present

The deceleratory gas uptake reaction was approximately represented by Eq. (2), though the rates were somewhat more rapid than the $FeS+SO_2$ reaction. Reaction proceeded apparently to completion, though removal of the cold trap showed that there was substantial condensation of SO_2. These results are consistent with the occurrence of an overall reaction that proceeds at a rate similar to that of the $FeS+SO_2$ reaction, but is accompanied by sulphur oxidation with subsequent condensation of the SO_2 formed.

3.4.3. FeS previously reacted with SO_2: No 78 K trap

Two consecutive reactions of FeS at 680 K are shown in Fig. 6. The first reaction (•) with SO_2 proceeded to completion at ~1050 min. Following evacuation of unreacted SO_2, oxygen was admitted and a second reaction was observed (•), again deceleratory and proceeding at a slightly slower rate. Introduction of a 78 K trap at 180 min resulted in the pressure dropping to zero at 250 min, attributed to conversion of the remaining oxygen to SO_2 by a rate process occurring during 180–240 min, followed by condensation. Subsequent removal of the cold trap resulted in a pressure rise corresponding to conversion of ~40% of the O_2 admitted to SO_2. Other experiments confirmed the occurrence of comparable behaviour at temperatures down to 560 K. Separation of the kinetic properties of the two or more reactions proceeding was not possible with the present apparatus.

3.4.4. Comment

These observations confirm that oxidation of a proportion of the sulphur in the FeS or Fe_2S_3 to SO_2 occurs at 680 K and below. Subsequent reactions may then proceed as already described and at a similar

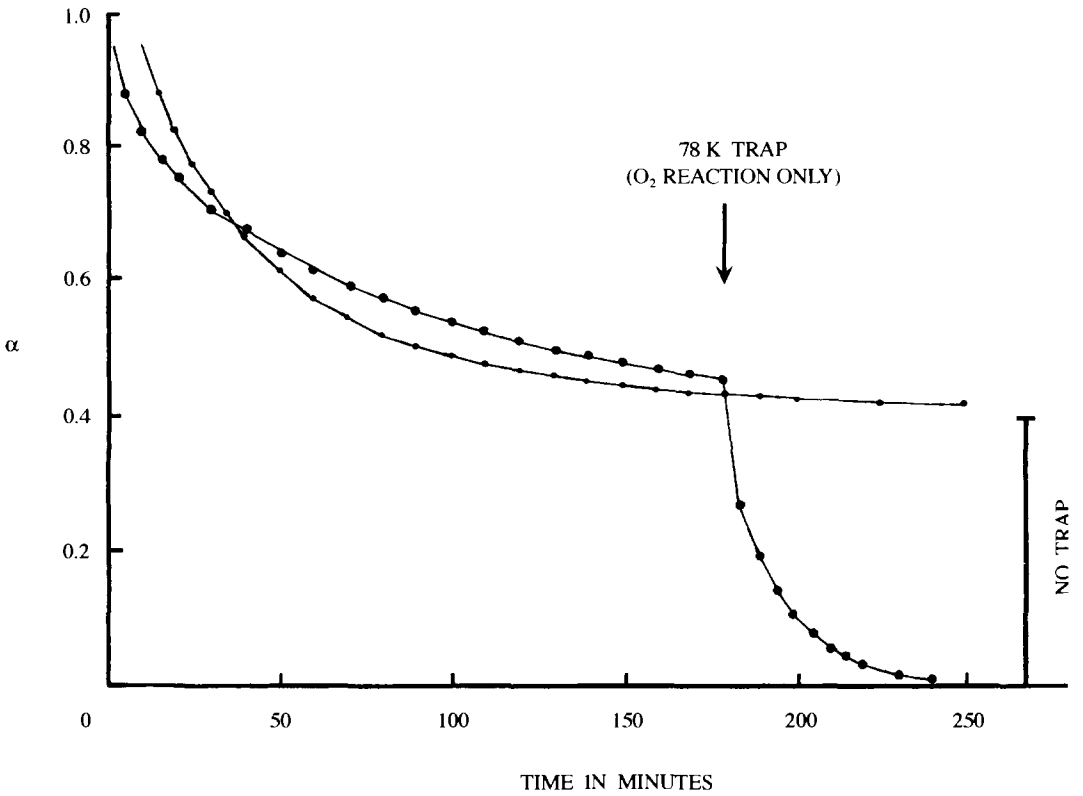

Fig. 6. The α–time plots for two consecutive reactions of FeS at 680 K: first with (•) SO_2 then, after evacuation, with (•) O_2. Introduction of a 78-K cold trap towards completion of the second rate process resulted in extensive condensation of a gaseous product. On removal of this cold trap, the pressure increase corresponded to volatilization of ~40% of the oxygen originally introduced, which had reacted to form SO_2.

rate. The evidence is consistent with partial oxidation of iron below the temperature at which $FeSO_4$ formation has been described [3]. Kinetic studies were not completed. Under the present conditions, it is expected that diffusion limitations within the interparticulate channels of the reactant powder will ensure a high local SO_2 concentration in the immediate vicinity of the reactant solid. Such conditions are not suitable for detailed kinetic studies of concurrent reactions.

3.5. Reaction of pyrites, FeS_2 with SO_2

No evidence of any reaction of pyrites, FeS_2+SO_2 was obtained from experiments between 650–720 K. Dunn et al. [13] detected the onset of reaction between pyrites and air to yield $FeSO_4$ and Fe_2O_3 at ~700 K. A series of reactions is proposed to explain their observations that includes the intervention of $Fe_2(SO_4)_3$ and sulphate decomposition to Fe_2O_3 [1,13].

3.6. Reaction of reduced iron with SO_2

The rate of reaction of iron powder (reduced) with SO_2 at 670 K was significantly slower (0.05 times) than that of FeS under similar conditions and the reaction with oxygen was even slower (0.002 times). This reactivity was lower than expected [14] and may be the result of superficial oxidation of this iron sample during storage.

3.7. Reactions of SO_2 with other selected solids

To determine whether the present reaction was a specific property of iron sulphide, only a few preliminary experiments were made for selected reactions using the above-mentioned conditions. The significant results are summarized below.

3.7.1. Metals

Deceleratory reactions, generally similar to that described above for $FeS+SO_2$, occurred between SO_2 and *zinc metal* above 680 K and between SO_2 and *nickel metal* above 660 K. The latter process was inhibited by oxygen. No perceptible reaction was detected between SO_2 and *silver metal* (24 h at 685 K) or *copper metal* (44 min at 680 K).

These oxidation reactions with SO_2 are therefore identified as metal specific, are not restricted to iron and can occur with other transition metals as well. Copper and silver may not be sufficiently electropositive to promote SO_2 dissociative adsorption at these reaction temperatures.

3.7.2. Sulphides

Neither Ag_2S nor PbS reacted significantly with SO_2 during 18 h at 680 K, though the latter sublimed some sulphur. HgS was sublimed from the heated zone without evidence of reaction.

3.8. Stoichiometric and mechanistic discussion of the $FeS+SO_2$ reaction

Both kinetic and microscopy complementary evidences are entirely consistent with the view that this reaction proceeds according to the theory of parabolic oxidation [11], originally developed by Wagner [12]. The reaction is initially rapidly established across all surfaces. The rate of subsequent advance of the reactant/product interface at which chemical change occurs is controlled by a diffusive transport process across the increasing thickness of the barrier layer of product. The overall rate of change in a reactant assemblage composed of equidimensional particles requires consideration of two controls. These are the ease of movement of the migrating entity within the solid–product phase together with the systematic reduction of the area of reactant–product contact according to the contracting cube model. These controls are combined in the Jander expression [1] which very satisfactorily represents the α–time data (Fig. 5). The sieved particles of the present reactants were in defined size ranges and the relative rates of reaction were in accordance with expectation from Eq. (2). Deviations were attributable to contributions from onset of intraparticulate reaction within the cracks and pores of the largest reactant particle sizes. Strong support for this interpretation of the kinetic results is provided by the microscopy observations in Figs. 2 and 3. A boundary, adherent layer of retextured material, a product phase, forms the outer zone of incompletely reacted particles. The composition of this product, the identity of the migrating species and the role of the two solid products mentioned in Eq. (1) must be discussed with reference to the reaction stoichiometry. Although the reaction model identified here is the same as that most successfully applied in metal oxidations [11,12], the chemistry of the present process shows significant differences that require further theoretical consideration.

3.8.1. Reaction stoichiometry

The reactions reported by Mellor [3] as occurring above 770 K ($FeS+2SO_2 \rightarrow FeSO_4+S_2$, followed by $4FeSO_4+S \rightarrow 2Fe_2O_3+5SO_2$) are different from the rate process already described and were studied here in the significantly lower temperature range, namely 560–700 K. The latter was accompanied by no sublimation of sulphur and Fe_2O_3 formation was not detected. Moreover, the gas uptake (Eq. (1)) was insufficient to convert the sulphide to sulphate, representing α=0.065 or 0.17, based on the first and the overall reactions mentioned here [3], respectively. It also seems probable that the large volume change expected from $FeS \rightarrow FeSO_4$ (estimated $\times$(2.5–3.0) from density values [15]) would result in product particle disintegration, which was not observed (Figs. 1–3). The temperature of onset of $FeSO_4$ decomposition, 748 K [1], is above the range of the present studies. We conclude, therefore, that the reaction reported here is novel and has not previously been described in the literature.

Equation (1) provides a satisfactory representation of the present stoichiometric observations. It also agrees with theoretical expectation for iron oxidation and sulphur accommodation in 0.38 Fe_2S_3, accompanied by partial oxidation of the remaining iron to 0.07 Fe_3O_4. However, mechanistic discussions must then proceed in the context of the relatively limited knowledge of the physical and chemical properties of Fe_2S_3.

Ferric sulphide is formed by reactions Fe+S [8] or FeS+S [9] at ~720 K, close to the present reaction temperature. (This compound can also be prepared by precipitation from solution [9].) At lower temperatures (333 K [9]) the decomposition Fe_2S_3 → FeS+FeS_2 is completed in a few hours. The formation of Fe_2S_3 in the present reaction can be explained by dissociative adsorption of SO_2, followed by irreversible accommodation of oxygen as Fe_3O_4, together with retention of released sulphur in Fe_2S_3 [3]. (In the absence of O_2, Fe_3O_4 is not oxidized to Fe_2O_3.) Assuming the heat of formation of Fe_2S_3 to be similar to that of FeS [15], we estimate the enthalpy of reaction (1) to be about -30 kJ mol^{-1}.

Fe_2S_3 is identified as the barrier layer and Fe^{3+} as the migrant species in the reaction expressed by Eq. (1). These conclusions are suggested by the following observations. The replacement of 1.00 FeS by 0.38 Fe_2S_3 is calculated, using listed densities [15], to be accompanied by a volume reduction of less than 1%. This product may replace the reactant from which it was derived with little structural reorganization. Yamaguchi and Wada [16] (see also [17]) describe Fe_2S_3 as a cation deficient structure, represented as $Fe^{3+}(\square_{1/3}Fe^{3+}_{5/3})S_4$ (similar to γ-Al_2O_3). This suggests that the present reaction is controlled by the rate of cation diffusion in the *vacancy rich* Fe_2S_3 structure. The migrant species is identified as Fe^{3+}, the smallest participating ion, with ionic radius 0.064 nm (smaller than Fe^{2+}, O^{2-}, S^{2-} [15]) and moves between the larger (radius 0.184 nm) immobile sulphide ions.

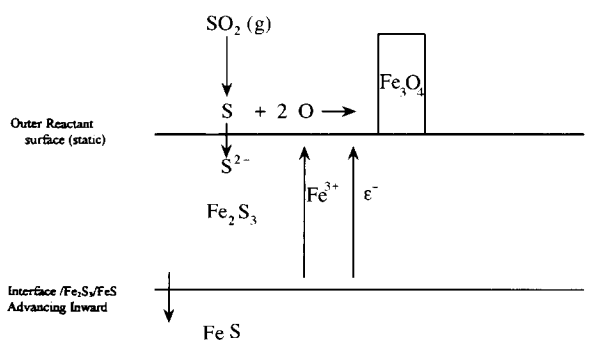

Scheme 1. Proposed Mechanism for Reaction FeS+SO_2

This reaction is summarized in a diagrammatic form in the scheme which extends the previous theory of oxidation reactions [11] to include here the involvement of a sulphide–barrier product phase. The SO_2 dissociative adsorption is suggested from comparisons with the facile rupture of S–O bonds, believed to occur during the oxidations of CaS and $CaSO_3$ [6] at a somewhat higher temperature. It is also consistent with the FeS+$2SO_2$→$FeSO_4$+S_2 reaction reported by Mellor [3]. Here the irreversible retention of the oxygen in Fe_3O_4 represents ~69% of the iron (Fe^{3+}) crossing the barrier layer. The open porous texture of the reacted solid (Fig. 1) suggests topotactic control of this product crystal growth (Fig. 1) – this phase, responsible for interparticle cohesion, becomes detached on crushing (Fig. 2). The remaining adsorbed sulphur is reduced to S^{2-} and forms Fe_2S_3, the greater proportion of which (87%) is generated within the particle at the advancing interface. The small difference between the observed and theoretical equations given in the Scheme 1 is readily explained by the expected deviation from stoichiometry of the reactant FeS [18]. While the properties of Fe_2S_3 have not yet been comprehensively characterized, its formation at reaction temperature has been reported [8,9] and the proposed mechanism is consistent with its expected properties [16].

The rate constant (k) for the FeS+SO_2 reaction at 625 K was 0.7×10^{-14} m^2 s^{-1}. Reported [19–22] values for the reactions of oxygen were with Hagg carbide (Fe_5C_2) – $10^{-14.7}$–$10^{-15.9}$ m^2 s^{-1}, cementite (Fe_3C) – $10^{-16.4}$–$10^{-17.5}$ m^2 s^{-1} and iron (Fe) – 10^{-19} m^2 s^{-1}. Reactivities, for these oxidations (O_2) which are controlled by diffusion across a Fe_3O_4 barrier (at least in the early stages), are in the sequence Fe_5C_2>Fe_3C>Fe. The present reaction proceeded more rapidly, consistent with expectation for Fe^{3+} transport control within a solid containing the larger immobile anions (radii: O^{2-} – 0.132, S^{2-} – 0.184 nm). Furthermore, the activation energy (75 kJ mol^{-1}) is

lower than the reactions involving Fe_3O_4 [19], 100 kJ mol^{-1}.

The formation of Fe_3O_4 as a product phase on the outer surfaces of reactant particles explains the change from the loose powder reactant to the hard pellet of residual solids. Generation of this oxide at particle contacts presumably acts as a coherent filler between, and bonded to the neighbours from which it was formed, yielding a rigid but porous matrix. Crushing resulted in fragmentation and detachment of this interparticulate bonding structure, changing the outer textual appearance (cf. Figs. 1 and 2).

3.9. $FeS+O_2$ reaction

The limited kinetic studies of this reaction, $FeS+O_2$, were both incomplete and unsatisfactory in that measurements of pressure changes did not detect sulphur oxidation $[S]+O_2 \rightarrow SO_2$. Moreover, the influence of diffusion limitations within the fine interparticulate pores of the reactant during chemical changes of the undoubtedly inhomogeneous mixtures of gaseous reactants (O_2+SO_2) must diminish the reliability of the kinetic data. The present observations are, nevertheless, of qualitative interest, pressure reductions result from the reactions of O_2 or SO_2 with the solid. Experiments with the 78 K trap provides strong evidence that sulphur, derived from the reactant FeS, is oxidized to SO_2 under these reaction conditions. Thus, gas uptake can be ascribed to the FeS-SO_2 reaction, explaining the kinetic results. It is also noted that the presence of oxygen did not inhibit reaction of this solid, a behaviour that contrasts with that found for nickel metal.

3.10. Flue-gas desulphurization

Any reaction capable of removing SO_2 from the products of coal combustion warrants consideration of its potential merit in contributing towards the reduction of acid rain. The present work has identified a strong affinity between FeS and SO_2 in the 560–700 K range. This reaction occurs most rapidly in the early stages and the efficiency of SO_2 uptake could probably be significantly improved by using a high area reactant preparation to minimize the opposition by solid product formation. An advantage of the process is that the residue is non-polluting, the less-familiar Fe_2S_3 soon decomposes to $FeS+FeS_2$ [9].

More work is, however, required to establish the value of this reaction, here subjected to the mechanistic study only, for flue-gas desulphurization. Problems requiring further investigation include determination of the ease of the reaction of sulphur from FeS with oxygen to yield SO_2, reversing the desired effect. Variations of the relative contributions of these rate processes (i.e. SO_2 formation and removal) with temperature would be required to determine whether a useful efficiency of SO_2 removal could be achieved. This could necessitate temperature controls in desulphurization to fine tolerances, perhaps to limits that are unrealistic in commercial equipment. The effects of other combustion products, nitrogen oxides, carbon oxides and others on this reaction would also require investigation. Perhaps this reaction, reported here as being of some theoretical interest in extending the range of rate processes identified as being controlled by diffusion across a barrier product layer, may have potential for combatting environmental pollution.

References

[1] M.E. Brown, D. Dollimore and A.K. Galwey, Comprehensive chemical kinetics, Vol. 22, Elsevier, Amsterdam, 1980.
[2] A.K. Galwey, J. Thermal Anal., 41 (1994) 267; Thermochim. Acta, 269/270 (1995) 621; Pure and Appl. Chem., 67 (1995) 1809.
[3] J.W. Mellor, Comprehensive treatise on inorganic and theoretical chemistry, Vol. 14, Longmans, London, 1935, p.160.
[4] D.C. Anderson, P. Anderson, A.K. Galwey, Fuel, 74 (1995) 1018, 1024.
[5] D.C. Anderson and A.K. Galwey, Fuel 74 (1995) 1031.
[6] D.C. Anderson and A.K. Galwey, Proc. R. Soc. London, A452 (1996) 585, 603.
[7] N.J. Carr and A.K. Galwey, Proc. R. Soc. London A404 (1986) 101.
[8] Gmelins Handbuch der Anorganischen Chemie, Verlag Chemie, Weinheim, Iron B2, 1930, p.372ff.
[9] E.de B. Barnett and C.L. Wilson, Inorganic chemistry, Longmans Green, London, 1953, pp.199–200.
[10] A.K. Galwey and M.E. Brown, Thermochim. Acta 269/270 (1995) 1.
[11] T.B. Grimley, Chemistry of the solid state, W.E. Garner, (Ed.), Butterworth, London, 1955, Chap. 14.
[12] C. Wagner, Z. Phys. Chem., 21 (1933) 25; 32 (1936) 447.
[13] J.G. Dunn, W. Gong and D. Shi, Thermochim. Acta 208 (1992) 293.

[14] J.W. Mellor, Comprehensive treatise on inorganic and theoretical chemistry, Vol. 13, Longmans, London, 1935, p.327.
[15] CRC Handbook of Chemistry and Physics, R.C. Weast, (Ed.), 62nd edn., CRC Press, Boca Raton, 1981–1982.
[16] S. Yamaguchi and H. Wada, Z. Anorg. Allg. Chem., 397 (1973) 222; J. Appl. Phys., 44 (1973) 1929.
[17] C. Sugiura, J. Chem. Phys. 74 (1981) 215.
[18] N.V. Sidgwick, The chemical elements and their compounds, Clarendon, Oxford, 1959, p.1329.
[19] J. Freel, B.R. Wheeler and A.K. Galwey, Trans. Faraday Soc. 66 (1970) 1015.
[20] W.E. Boggs, R.H. Kachik and G.E. Pellissier, J. Electrochem. Soc., 112 (1965) 539; 114 (1967) 32.
[21] E.A. Gulbransen, Trans. Electrochem. Soc., 81 (1942) 327; Ind. Eng. Chem., 41 (1949) 1385.
[22] E.J. Caule, K.H. Buob and M. Cohen, J. Electrochem. Soc. 108 (1961) 829.